FINAL COPY

An Improved Optical Spectrum and New Model Fits of the Likely Brown Dwarf GD 165B

J. Davy Kirkpatrick

Infrared Processing and Analysis Center, M/S 100-22, California Institute of Technology, Pasadena, CA 91125; davy@ipac.caltech.edu

France Allard

Centre de Recherche Astrophysique de Lyon, Ecole Normale Supérieure de Lyon, F-69364 Lyon Cedex 07, France

Tom Bida

W. M. Keck Observatory, 65-1120 Mamalahoa Highway, Kamuela, HI 96743

Ben Zuckerman and E. E. Becklin

Department of Physics and Astronomy, University of California, Los Angeles, CA 90095-1562

and

Gilles Chabrier and Isabelle Baraffe

Centre de Recherche Astrophysique de Lyon, Ecole Normale Supérieure de Lyon, F-69364 Lyon Cedex 07, France

ABSTRACT

Long thought by some researchers to be an oddity, **GD 165B** has instead proven to be the first example of a class of very cool objects (the **L dwarfs**) which, due to dust formation in their photospheres, lack the dominant bands of TiO seen in warmer M dwarfs. Here we present an improved optical (6200–10300 Å) spectrum of GD 165B and identify its prominent spectral features. Among these are newly identified bands of **FeH** and the first identification of **CrH** bands in a dwarf. We use the latest generation of model **atmospheres**, which include the effects of **condensation** and **dust opacities**, to derive values of T_{eff} = 1900±100K and log(g) = 5.0±0.5 for GD 165B. We also derive a crude age of 1.2 to 5.5 Gyr for the GD 165 system. A comparison of the temperature and age of GD 165B to evolutionary models predicts GD 165B to be an object in the transition zone between stars and brown dwarfs. Further observational evidence – the discovery of lithium in other dwarfs spectroscopically similar to GD 165B and the scarcity of GD 165B-like companions found by imaging surveys – favors a substellar interpretation for this object. We argue that the weight of this observational evidence together with the known shortcomings of the evolutionary models (which do not yet include opacity by grains) indicate that GD 165B is probably a **brown dwarf**.

Subject headings: stars: atmospheres — stars: individual (GD 165B) — stars: low-mass, brown dwarfs

1. Introduction

Just a few months ago Gl 229B, at 5.7 pc, was the only uncontested brown dwarf known in the immediate vicinity of the Sun. Now, however, several new brown dwarfs and brown dwarf candidates have been added to the nearby substellar census. Kelu-1, discovered during a proper motion survey (Ruiz et al. 1997), is estimated to be at 10 pc. DENIS-P J1228.2-1547, DENIS-P J1058.7-1548, and DENIS-P J0205.4-1159 — all discovered photometrically by the DEep Near-Infrared Survey (DENIS) — are similar to, or cooler than, Kelu-1 and presumably lie within ~20 pc of the Sun (Delfosse et al. 1997). DENIS-P J1058.7-1548, the warmest of the DENIS trio, shows no lithium in its spectrum, but DENIS-P J1228.2-1547 and Kelu-1 do (Tinney et al. 1997; Martín et al. 1997; Ruiz et al. 1997). DENIS-P J0205.4-1159 does not show lithium at low resolution (see spectrum in Tinney et al. 1997) but is even cooler and redder than DENIS-P J1228.2-1547. Kelu-1 and DENIS-P J1228.2-1547 appear to be ~1-Gyr-old objects falling at the upper-mass end of the so-called "lithium brown dwarfs", meaning that they are brown dwarfs with less than ~0.060 $M_\odot$. Presumably, objects of similar age which are slightly warmer and which lack the lithium signature could also be brown dwarfs with masses in the range 0.060 $M_\odot < M < 0.075\ M_\odot$. Two other hotter, and presumably younger, field objects have also been recently confirmed as lithium brown dwarfs — the ≥M9 dwarf LP 944-20 (Tinney 1998b, age ~0.5 Gyr) and perhaps the M6 dwarf SERC 296A (Thackrah et al. 1997, age ~0.02 to 0.2 Gyr).

Curiously, each of the ~1-Gyr-old objects have optical spectra (Ruiz et al. 1997; Tinney et al. 1997) very similar to the brown dwarf candidate GD 165B, discovered almost a decade ago (Becklin & Zuckerman 1988) and first observed spectroscopically a few years later (Kirkpatrick et al. 1993a). In light of these new discoveries, the investigation into the nature of GD 165B should be reopened. In this paper we present a much improved optical spectrum obtained with the 10-meter Keck telescope and compare it to much improved atmospheric models which now include the effects of condensation and dust opacities.

2. Data Description

2.1. Observational Details

GD 165B was observed on two occasions in the spring of 1995 utilizing the Low Resolution Imaging Spectrograph (LRIS, Oke et al. 1995) at the W. M. Keck Observatory. A first set of observations was conducted on UT 1995 Mar 30 (hereafter, "Set-1") followed by another set at shorter wavelength on UT 1995 May 08 (hereafter, "Set-2").

The Set-1 observations were conducted as follows. A 600 g/mm grating blazed at 7500 Å along with a 1.″0 slit were used to produce a first-order spectrum covering the range 7588–10308 Å with an effective resolution of 5 Å (4-pixel projected slit, 1.28 Å/pixel dispersion). The GD 165AB pair was acquired on the slit-viewing guider of the LRIS, with both components being visible in a 5-sec guider exposure. The position angle of the slit was set to 191°, matching the binary position angle given in Zuckerman & Becklin (1992), so that both objects could be observed together. Simultaneous spectra were obtained at this fixed angle, and another star in the acquisition field was used for guiding. Four successive 1500-sec exposures were taken, interspersed with internally illuminated quartz flat-field and emission-arc spectra. The observing conditions included intermittent cloudiness, as evidenced by variation in the measured flux of the objects from frame to frame. Local seeing was approximately 0.″85 FWHM.

The Set-2 observations were conducted with the instrument rotated to a position angle of 101°. In this case, the bright primary GD 165A was located normal to the slit and was used as the control-loop guide star. The 600 g/mm grating was used to cover the range 6160–8760 Å at 5 Å resolution. A single 1200-sec exposure was taken under clear observing conditions, and the seeing was approximately 1.″1. Internally-illuminated calibration exposures were also taken. In addition, a 100-sec exposure of the flux standard G 138-31 was acquired at the same setting but through a wide-open 8.″5 slit.

One additional observation completed the data set. Two exposures, of 10 sec and 20 sec, were taken of the flux standard G 191-B2B on UT 1996 Apr 24. This observation, taken with the same spectrograph settings as Set-1 but through the 8.″5 slit, was used to perform a relative flux calibration for the longer wavelength spectrum of GD 165B.

2.2. Data Reduction

The IRAF spectral reduction package was used to extract and calibrate all of the program spectra. The LRIS CCD was operated in dual-amplifier readout mode for each of these observations except for the final G 191-B2B set. For reduction purposes this means that each half of the 1024-column data set was extracted and calibrated separately so that the appropriate CCD system gain and noise characteristics of the individual readout amplifiers could be applied to each extraction.

Reductions were done as follows. The overscan region of the CCD readout was averaged over rows, fit with a cubic spline function, and subtracted from each amplifier region. After overscan subtraction, flatfield spectra were trimmed, combined, normalized, then divided into each stellar spectrum. Due to non-negligible instrumental rotational flexure, combined with significant fringing patterns of up to 10% variability in the images at these red wavelengths, it was imperative to flatten the object spectra with flatfields taken in direct sequence with them. These flatfields reduced the fringing variations to the 1.5% level.

The Set-1 GD 165B spectra, only 17 pixels (3.″7) away spatially from the spectra of the primary, required special attention at this step. The spatial background at each wavelength was interactively fit with a fourth-order polynomial and subtracted from the object spectrum (in the optimal extraction scheme of Horne 1986). Using this method spectral contamination from the primary was minimized.

The resulting GD 165B and standard star spectra were dispersion corrected using polynomial fits to the arc spectra extracted from the same spatial trace as each object spectrum. The instrumental response was computed from the standard star observations using tabulated flux values in Oke (1974, 1990). Finally, the GD 165B spectra were extinction corrected with tables derived for Mauna Kea as supplied by Stockton (1996) and flux calibrated with the resulting standard star sensitivity functions.

As mentioned previously, the Set-1 spectra were affected by variable sky transparency. Only one of these spectra is used further because the others were found to have insufficient signal-to-noise to add meaningfully to the data. The integrated signal-to-noise of this single spectrum is about 33-to-1 in the continuum at 8250 Å adjacent to the Na I doublet. The Set-2 spectrum by comparison yielded signal-to-noise values of about 35-to-1 in the same region.

2.3. Piecing the Spectra Together

Published spectra for GD 165B cover the optical and near-infrared regions. The two spectra described above cover 6160 to 10308 Å, and the spectrum of Jones et al. (1994) covers 1.14 to 2.49 μm. The only one with absolute flux scaling is the short-wavelength optical portion; the other optical spectrum was taken in non-photometric conditions. The spectrum of Jones et al. was normalized to unity, losing any absolute normalization. In any event, there is no mention in their paper as to whether the conditions were photometric, so absolute scaling on this piece would be suspect.

In order to produce a long-baseline spectrum with the correct normalizations, we have done the following. Because the Set-2 spectrum was taken under photometric conditions, the overlap region (from 7588 to 8760 Å) between this spectrum and the Set-1 spectrum was used to fix the absolute normalization of the Set-1 portion (simply by multiplying the flux scale by a constant). The resulting 6160–10308 Å spectrum is shown in Figure 1.

Because there is no overlap between the optical spectra and the Jones et al. spectrum, the latter was normalized using existing infrared photometry. Specifically, the Jones et al. spectrum was multiplied by a constant so that the resulting JHK magnitudes would match published values by Becklin & Zuckerman (1988) and Tinney et al. (1993). This near-infrared piece was also converted from F_ν (as given in Jones et al.) to F_λ to match the units used in the optical. The resulting, absolutely-fluxed spectrum from the optical through the near-infrared is shown in Figure 2.

The absolutely-fluxed spectrum of Figure 2 can be convolved with I, J, H, and K filter transmission functions, resulting in the synthetic photometry listed in Table 1. (Because the Jones et al. spectrum is clipped off at the short-wavelength side of the J-band, the J magnitude is a little more uncertain than the others.) Table 1 also lists the published I, J, H, and K photometry. Jones et al. pieced their spectrum together from small spectral segments whose relative normalizations were set to match published photometry. The synthetic JHK magnitudes agree well with the published values, confirming that the Jones et al. normalizations of the spectral pieces are correct.

An argument *can* be made that the optical spectrum should be shifted upward by 0.2 mag (i.e., be made brighter) to match better the published I-band magnitude. After all, the absolutely-fluxed, 6160–8760 Å spectrum of GD 165B was taken through a narrower slit than was the flux standard[1], so the flux of GD 165B will have been somewhat underestimated. However, our derived value of I=19.44 is within the error of the published I measurement. Thus, further tweaking of the normalization in the optical is unwarranted.

3. Analysis

3.1. Feature Identifications in the Optical Portion

All features identified in the optical spectrum of GD 165B are listed in Table 2 and marked in Figure 1. Neutral atomic lines are addressed below first, followed by molecular bands.

3.1.1. Neutral Atomic Lines

The high gas pressure in the atmospheres of dwarfs drives easily ionized species toward lower degrees of ionization, and the low temperatures associated with GD 165B favor transitions of neutral atoms with the lowest ionization energies. Thus, neutral lines of alkali metals — Li, Na, K, Rb, Cs, and Fr — should be the most prevalent atomic lines. At the resolution and signal-to-noise of our GD 165B spectrum, the Li doublet at 6708 Å (upper limit to the equivalent width is 0.7 Å) and lines of Fr (an extremely unstable element with a half life of 22 min for the longest lived isotope) are not seen. However, all other atomic lines in the spectrum of GD 165B can be ascribed to one of the other four alkali metals:

Na I: The doublet at 8183, 8195 Å — one of the hallmarks of a dwarf luminosity class — is very strong.

K I: The resonance doublet at 7665, 7699 Å is seen as a very wide feature in the Figure 1 spectrum. This broadening has also been noted by Martín et al. (1997) in the spectra of the DENIS-P objects. The K I lines seen in late-M dwarfs, by comparison, are very distinct, narrow features.

[1]Observations of the flux standard also served another duty. These were used as a check of the absolute efficiency of LRIS, dictating that a wide-open slit be used.

Rb I: The resonance doublet at 7800, 7948 Å is present. The 7948-Å line is very strong and has also been seen, though much weaker, in late-M dwarfs observed at higher resolution by Basri & Marcy (1995). Both lines are seen in the spectra of the DENIS-P objects (Tinney et al. 1997).

Cs I: The resonance doublet at 8521, 8944 Å is present. The 8521-Å line is particularly deep and distinct. This line has also been seen, though much weaker, in late-type M dwarfs observed at higher resolution by Tinney (1998a). Both lines are strong in the optical spectra of the DENIS-P objects (Tinney et al. 1997) and the brown dwarf Gl 229B (Oppenheimer et al. 1998; Schwenke 1998).

3.1.2. Molecular Bands

In this wavelength regime, all of the observed molecular bands are caused by electronic transitions. Several of these bands are identified in cool dwarfs for the first time.

FeH: We have identified the (0-0) and (1-0) bands of the $A^4\Delta$–$X^4\Delta$ transition (Phillips et al. 1987; Schiavon et al. 1997). Both of these have a sharp head which degrades toward longer wavelengths. The (0-0) bandhead at 9896 Å, also known as the Wing-Ford band, is one of the dominant features in the spectrum of Figure 1. Clegg & Lambert (1978) and Wing et al. (1977) have positively identified the (0-0) band in the spectra of S stars, M giants, and K and M dwarfs, and Wing et al. (1977) have identified both the (0-0) and (1-0) bands in the spectra of sunspots.

CrH: A sharp band at 8611 Å, also seen in the spectra of late-M dwarfs, had been previously identified as part of the 8521–8668-Å band of VO. As shown in the spectra of Kirkpatrick et al. (1997), the other two VO bands of the same transition (see discussion on VO below) appear in the spectra of both late-M dwarfs and late-M giants. However, this supposed VO band near 8611 Å appears in dwarfs but *not* in giants. Additionally, unlike the other two VO bands, the 8611-Å feature has a distinct bandhead which degrades redward. Most likely, this is not VO but instead the "unidentified" band that Keenan (1957) found in the S-type star R Cygni. Although Lindgren & Olofsson (1980) were unable to observe the band in mid-M giant and mid-M dwarf spectra, they produced convincing evidence that the band in R Cygni was due to CrH. Concurrently, Engvold et al. (1980) positively identified this same band as CrH in a high-

resolution spectrum of a sunspot. Sauval (1978) notes that CrH should be found in M dwarfs since CaH and FeH are also seen. Our models also show that CrH should be as abundant as CaH and FeH. As seen in the cool spectra of Kirkpatrick et al. (1997) and Tinney et al. (1997), this band strengthens markedly with decreasing temperature, and as seen in Figure 1, is one of the strongest features in the spectrum of GD 165B. Given this evidence we, too, identify this band as CrH.

The 8611-Å feature corresponds to the (0-0) band of the $A^6\Sigma^+$–$X^6\Sigma^+$ transition (Pearse & Gaydon 1963). The (1-0) and (2-0) bands at 7642 and 6890 Å, if present, are coincident with the telluric A- and B-bands of O_2. CrH exhibits behavior very similar to that of the other hydride discussed here, FeH. Not only do the aforementioned (0-0), (1-0), and (2-0) bands of the $A^4\Delta$–$X^4\Delta$ transition of FeH appear in the optical spectrum of GD 165B, but also the (0-1) band of the same electronic transition of FeH appears in the Jones et al. near-infrared spectrum at 11939 Å. Likewise, the (0-1) band of the $A^6\Sigma^+$–$X^6\Sigma^+$ transition of CrH is seen in our far optical spectrum at 9969 Å.

TiO: Unlike the spectra of M dwarfs, the spectrum of GD 165B generally lacks recognizable bands of TiO. The only exception is the (0-0) band of the $E^3\Pi$–$X^3\Delta$ transition, with heads at 8432, 8442, and 8452 Å degraded redward. In late M dwarfs, this is the most dominant TiO band in the optical spectrum. In the spectrum of GD 165B, it is far weaker.

VO: In the far optical spectra of very late M giants (Kirkpatrick et al. 1997), there are three regions with broad, shallow VO absorption, each lacking a dominant bandhead. Specifically, these are all due to bands of the $B^4\Pi$-$X^4\Sigma^-$ transition: the (1-0) band between 7334–7534 Å, the (0-0) band between 7851–7973 Å, and the (0-1) band between 8518–8667 Å (Keenan & Schroeder 1952). Partly because of this lack of an obvious bandhead, however, the only one of the three that is clearly seen in the spectrum of GD 165B is the (1-0) band, though even this is blended with the blueward wing of the K I doublet. Furthermore, the (1-0) band of the $A^4\Pi$-$X^4\Sigma^-$ transition in the region ~9540–9630 Å is probably also present in GD 165B because the (0-0) band of the same transition (~10460–10562 Å, Spinrad & Wing 1969) is strong in the Jones et al. near-infrared spectrum. However, this (1-0) band is coincident with a telluric water feature, making its identification ambiguous.

Telluric bands of O_2 and H_2O: The remaining strong bands in the spectrum of Figure 1 are due to unremoved telluric features. The A- and B-bands of O_2 appear with strong heads at 7594 Å and 6867 Å, respectively. Bands of H_2O appear prominently in the regions ~8955–9225 Å, ~9279–9681 Å, and ~9701–9826 Å. Some of these water bands, particularly those near 9300 Å which arise from the $\nu_1 + \nu_3 = 3$ bands (Schwenke 1998), may in part result from steam in the atmosphere of GD 165B itself, but an observing program specifically designed to remove telluric features must be undertaken to state this with certainty.

3.2. Model Fits to the Entire Spectrum

The spectrum of GD 165B exhibits the same major features as a very late-type M dwarf (see spectra in Kirkpatrick et al. (1997)) *except* that it lacks the prominent bands of TiO. As such it is the prototype of the L dwarf class. In the latest generation of model atmospheres, this lack of TiO can be explained by dust formation at cool temperatures.

Allard et al. (1997) have reviewed the rapid progress in atmospheric models for lower main sequence stars and brown dwarfs. The importance of dust grain formation, its effects on the depletion of refractory elemental abundances, and its heating effects upon the photospheres of red dwarf stars have been revealed in greater detail. These processes have been shown to be responsible for the noticed transformations in the spectral characteristics of very cool objects compared to hotter M dwarfs (Tsuji et al. 1996; Jones & Tsuji, 1997; Allard 1998). Sharp & Huebner (1990) introduced the first comprehensive condensation calculations for high-density, low-temperature gas mixtures. Tsuji et al. (1996) applied these results for three grain species — iron (Fe), enstatite ($MgSiO_3$), and corundum (Al_2O_3) — to non-grey model atmospheres, and found an important reddening of the spectral distribution due to corundum opacities. For the first time the models provided a good match to the photometric properties of GD 165B and resulted in an estimate of T_{eff} = 1800K. Allard (1998) and Allard et al. (1998b) extended this type of computation to include the complete list of over 1000 crystals and liquids studied by Sharp & Huebner. The more detailed equation of state calculation led them to recognize that Ca silicates (e.g., $Ca_2Al_2SiO_7$), forsterite (Mg_2SiO_4) and iron — instead of corundum — were the leading opacity sources in late-type dwarfs. They also concluded that per-

ovskite ($CaTiO_3$) grains are those responsible for the depletion of TiO as observed here in GD 165B. These models also predict the partial depletion of all refractory elements (especially Ca, Al, Si, Mg, Ti, Fe, Ni, V, and Zr) from the atmospheres of red dwarfs at the bottom of the main sequence.

It is these NextGen-dusty models (see Allard et al. 1998a) which we use here to derive the atmospheric parameters of GD 165B. The models are constructed using an opacity sampling technique and a complete opacity database including the latest H_2O and TiO line lists by Partridge & Schwenke (1997) and Jørgensen et al. (1994) and opacity profiles for 12 grain species reconstructed from their polarizability spectra. These models show a strong sensitivity to changes in effective temperature and gravity in the near-infrared (J to K bandpass) region. This allows a robust determination of T_{eff} = 1900±100K and log(g)= 5.0±0.5 for GD 165B if a solar metallicity is assumed in the pre-condensation model. This best fit, shown in Figure 3, provides an excellent match to the overall spectrum. This is unprecedented because grainless models have traditionally overestimated the strengths of water vapor absorption bands in this regime by as much as 2 magnitudes. Our determination of T_{eff} = 1900K is slightly warmer than the 1800K value of Tsuji et al. (1996), who failed to reproduce the I-to-J band spectral region adequately. In our model, the details of the H_2O and CO bands are well reproduced, with H_2 opacities shaping the red wing of the K-band flux peak at 2.0-2.2 μm. CH_4 bands at 1.6 and 2.4 μm that would confirm a substellar nature for GD 165B are not detected.

This remarkable agreement with the general spectral distribution and colors should not at this point inspire great confidence in the precision of the derived parameters, however. A quick look at the optical spectral region in Figure 4 reveals that the same model does not reproduce accurately the distinctive optical features in cool dwarfs like GD 165B. Indeed, the model fails to explain the observed depletion of VO and still predicts TiO bands that are too strong. It also underestimates the strengths of the observed Cs I lines which appear due to the relative lack of Cs depletion. The lack of VO and TiO depletion and the weakness of Cs I and other atomic lines of unrefractory elements reflects the shortcomings of the current models which assume that the grains remain suspended at the condensation level. This assumption is clearly wrong since gravitational pull on large metallic grains should be quite efficient in these high gravity dwarfs. Preserving the grains at their condensation heights causes the upper photosphere in the models to be too hot, due to backwarming induced by grain opacities. The correction for this effect in later models should also correct the underestimation of the TiO and VO depletion and the underestimation in core strength of strong atomic lines. Nevertheless, the general continuum is far better reproduced than in grainless models (see, for example, Kirkpatrick et al. 1993b), and these latest results constitute a major step forward in the continuing progress seen in brown dwarf model atmosphere development.

One interesting point is that despite its very complete opacity database, the model does not predict a feature in the 8611-8800 Å spectral region. The fact that CrH opacities are not included in the model databases, and that the CrH molecule is just as abundant as the other important metal-hydride absorbers (e.g., FeH) included in our models, further supports the claim that these observed bands are caused by CrH.

4. Discussion

4.1. Theoretical Considerations

Can any conclusion be drawn on whether or not this object is a brown dwarf? Yes, but given our temperature determination of 1900±100K, the age must also be estimated. Fortunately, the white dwarf primary star provides some important clues. Bergeron et al. (1995), using new model atmospheres and synthetic spectra along with improved mass-radius relationships for ZZ Ceti stars, calculate a white dwarf mass for GD 165A of 0.56-0.65 $M_\odot$ and a temperature of 12000-13000K. Measurements of white dwarfs in star clusters of known age give a coarse relation between main sequence mass and mass of the resulting white dwarf. Bragaglia et al. (1995) argue for a relation agreeing with the semi-empirical result of Weidemann (1987), which is shallower than the linear relation of Iben & Renzini (1983) and better able to predict the peak in the observed white dwarf mass distribution[2]. For a white dwarf of mass 0.56 $M_\odot$, Weidemann's relation predicts an initial mass of 1.2 $M_\odot$. Similarly, for a white dwarf of mass 0.65 $M_\odot$,

[2]Reid (1996), however, casts doubt on the uniqueness of the relation between initial and final masses, suggesting that mass loss rates vary markedly for progenitors of similar mass.

the relation gives a progenitor mass of 3.0 $M_\odot$.

With the initial and final mass estimates in hand, we can now use stellar evolutionary theory to predict the age of the GD 165 system. Using the stellar lifetime calculations of Scalo (1986), we find that a 1.2-$M_\odot$ star and a 3.0-$M_\odot$ star will spend ~4.6 Gyr and ~0.4 Gyr, respectively, on the main sequence. Compared to the amount of time spent on the main sequence, the amount of time spent in the giant phases is much shorter and can be neglected. Finally, the time taken for a ~0.6-$M_\odot$ white dwarf to cool to 12000 K is between ~0.65 Gyr and ~0.85 Gyr (Segretain et al. 1994). Thus, the age of GD 165A, and hence of GD 165B, is less than 5.5 Gyr but more than 1.2 Gyr.

This age computation, however, is further complicated by the recent discovery of Saffer et al. (1998) that the white dwarf primary itself is a spectroscopic binary. No lines from this third component (which we will dub "GD 165C") are seen in the spectrum of GD 165A, meaning that "C" is most likely an even cooler white dwarf. The white dwarf referred to as "A", because it is warmer, must have formed after the "C" component since it has had less time to cool. Since the amplitude of the radial velocity variations suggests that this white dwarf pair is also a very short period binary, there is a chance that the system underwent mass transfer when the progenitor of the "C" component left the main sequence, possibly filling its Roche lobe (see Iben et al. 1997). This would have increased the mass of the main sequence progenitor of the "A" component, causing the progenitor to leave the main sequence sooner than it should have. In our preceding calculation, the resulting white dwarf mass of "A" would thus be extrapolated back to a main sequence progenitor which had already seen mass transfer from its companion. The deduced age would thus be too small since it does not adequately reflect the amount of time that the less massive "A" progenitor spent on the main sequence prior to the mass transfer phase. In summary then, the true age of the system may be older than our estimate.

GD 165B can be plotted on the theoretical T_{eff} vs. age diagram and compared to the latest evolutionary tracks for brown dwarfs and low-mass stars. Figure 5 shows the location of GD 165B relative to the latest models by Chabrier & Baraffe (1997) and Baraffe et al. (1998). These models use Allard's NextGen model atmospheres. Although grain formation is known to play a significant role in the emergent spectrum of GD 165B, grain effects have yet to be included in the Chabrier/Baraffe models. With this caveat in mind, Figure 5 suggests that GD 165B is most likely a transition object. In these models a "transition" object is defined as a dwarf having a mass below 0.075 $M_\odot$ but above 0.072 $M_\odot$. The models show that objects with masses above 0.075 $M_\odot$ achieve core hydrogen burning and are stars. Objects below 0.072 $M_\odot$ never achieve core hydrogen burning and are thus brown dwarfs. Objects in between have not stabilized on the main sequence even for ages of 10 Gyr but may eventually achieve core burning at ages greater than a Hubble time. It is these ambiguous cases that we refer to as "transition" objects, and the models suggest that GD 165B warrants such a designation.

Independently of the temperature determination, we can plot GD 165B on the M_K vs. age diagram of Figure 6. Again, GD 165B falls squarely in the stellar/substellar transition region. As shown by the dashed lines in both figures, however, an object like GD 165B with age > 1.2 Gyr and inferred mass between 0.065 and 0.075 $M_\odot$ should already have destroyed its lithium whether or not it is really a brown dwarf.

4.2. Observational Considerations

Despite the fact that the theoretical plots support a transitional nature for GD 165B, other observational evidence suggests that it is a brown dwarf. GD 165B was discovered during a companion search around 200 nearby white dwarfs (Zuckerman & Becklin 1992) and this search uncovered 20 additional companions. All had $M_K < 10$ except for GD 165B itself. The relative numbers of companions in bins brighter than $M_K = 10$ are consistent with a mass function like that measured in the field ($\xi(M) = dN/d(log(M)) \propto M^{-\alpha+1}$ where $0.70 < \alpha < 1.85$ for $0.08M_\odot < M < 0.5M_\odot$, Kroupa 1998). If we take a best guess mass function with $\alpha = 1.0$, we find that the observed numbers of companions found by Zuckerman & Becklin in the logarithmically-equal intervals of 0.089-0.099 $M_\odot$ (5 companions) and 0.080-0.089 $M_\odot$ (4 companions) predict that ~4.5 companions should have been found in the 0.072-0.080-$M_\odot$ interval.[3] GD 165B alone occupies this lower mass regime. Because the survey is complete to $M_K = 12.0$, this lower mass bin is fully sampled except for possibly the very lowest masses ($< 0.073M_\odot$) at the very oldest ages (> 4 Gyr), so

[3]The relation given by Henry & McCarthy (1993) was used to convert M_K to mass.

objects are not being missed because of lack of sensitivity. Furthermore, as stated in their second footnote, Zuckerman & Becklin surveyed another ~100 white dwarfs and found another 10 low-mass stellar companions but no additional GD 165B-like objects. These numbers only make the discrepancy between observed and predicted values even more significant for the lowest mass bin.

We must conclude from this either that (a) GD 165B-type objects are stars and the stellar mass function plunges precipitously at $M_K \approx 10$, which seems aphysical, or (b) GD 165B-type objects are comprised at least partly of brown dwarfs. It should be noted here that the mass function for M dwarfs in the Pleiades cluster has $0.6 < \alpha < 1.0$ (see discussion in Bouvier et al. 1998). This demonstrates that on crossing the stellar/substellar boundary, the mass function continues with roughly the same slope as before. This rules out case (a). The observational discrepancy between the relative numbers of higher mass companions and the numbers of lower mass ones can thus be explained if the former is sampled from a main sequence mass function (where luminosities stabilize and remain constant for billions of years) and the latter sampled at least partly from a substellar mass function (where objects continuously cool, with the older counterparts dimming beyond detection limits).

A likely brown dwarf status for GD 165B is supported on other observational grounds as well. Four field dwarfs with spectra similar to GD 165B are now known, as discussed in §1. Kelu-1 and DENIS-P J1058.7-1548 show deeper TiO bands and are thus slightly warmer than GD 165B. The former shows a strong lithium line while the latter shows none. DENIS-P J1228.2-1547 and DENIS-P J0205.4-1159 show even less TiO than GD 165B presumably because their temperatures are lower. The first shows a strong lithium line while the second does not. In other words, 50% of known field objects with GD 165B-like spectra are lithium brown dwarfs. (Either the other 50% are a mixture of brown dwarfs with masses above ~0.060 $M_\odot$ and stars, or they are all brown dwarfs with masses above ~0.060 $M_\odot$.) This contrasts sharply with warmer field M-dwarfs where, despite a much larger census of objects, only two are known to have lithium. It appears then that field objects at $T_{eff} \approx 1900K$ come from a fundamentally different mix of objects than do these warmer dwarfs and that the percentage of such objects which are brown dwarfs in this regime is somewhere between 50 and 100%. This fact combined with the aforementioned scarcity of GD 165B-type companions strongly suggests that many such objects are substellar.

We conclude that GD 165B is likely a true brown dwarf. Considering the fact that the Chabrier/Baraffe models do not yet adequately include grain opacities, the disagreement between what theory and observation suggest as the true nature of GD 165B may vanish after the models are further refined. Better statistics on the frequency of lithium brown dwarfs in the GD 165B regime will come from follow-up of targets selected from the 2MASS and DENIS surveys. With the additional observational evidence these surveys will provide and with advances in the modelling of these objects, there is hope of more clearly understanding the nature of this object.

5. Conclusions

We have presented a new, higher signal-to-noise spectrum of GD 165B between 6200 and 10300 Å. This spectrum shows strong bands of CrH, FeH, and probably H_2O along with TiO and VO bands which are weakened compared to those in late-M dwarfs. Also strong are atomic lines of the neutral alkali metals Na, K, Rb, and Cs. Using the latest atmospheric models, we have estimated a temperature of 1900±100 K. Comparison with theoretical work along with an analysis of the observational evidence shows that GD 165B is likely a brown dwarf.

We are grateful to Hugh Jones for the use of his near-infrared spectrum, to David Koerner for a discussion on molecular spectroscopy, to Ben Oppenheimer for a chance to view his optical spectrum of Gl 229B prior to publication, to Chris Tinney for an on-going dialog into the spectral similarities between GD 165B and the DENIS-P objects, and to Rex Saffer and Jim Liebert for a discussion on the duplicity of GD 165A. Observations reported here were taken with the W. M. Keck Observatory, operated as a scientific partnership between the California Institute of Technology, the University of California, and the National Aeronautics and Space Administration. The Observatory was made possible by the generous financial support of the W. M. Keck Foundation. FA acknowledges NASA grants 110-96LTSA and NAG5-3435 to Wichita State University. The research described in this publication was partially carried out by

the Jet Propulsion Laboratory, California Institute of Technology, under a contract with the National Aeronautics and Space Administration.

TABLE 1
COMPARISON TO PUBLISHED PHOTOMETRY.

Band[a]	Magnitude from Fig. 2 spectrum	Magnitude from Tinney et al. (1993)	Magnitude from Becklin & Zuckerman (1988)
I_C	19.44	19.25±0.2	—
J_{CIT}	15.73	15.80±0.05	15.75±0.10
H_{CIT}	14.80	14.78±0.05	14.76±0.04[b]
K_{CIT}	14.15	14.17±0.05	14.09±0.04[b]

[a]Using the latest parallax measurement for GD 165A ($\pi_{abs} = 0\farcs0317\pm0\farcs0025$, Dahn 1997), these values yield absolute magnitudes for GD 165B of (M_I, $M_{J_{CIT}}$, $M_{H_{CIT}}$, $M_{K_{CIT}}$) = (16.95, 13.24, 12.31, 11.66).

[b]These magnitudes as published in Becklin & Zuckerman (1988) *are* on the CIT system despite what is implied by the footnote in their table.

TABLE 2

FEATURE IDENTIFICATIONS IN THE OPTICAL REGION.

Atom/Molecule	Location (Å)	Transition
VO	~7334–7534	1-0 band of $B^4\Pi$–$X^4\Sigma^-$
K I	7665	$4s^2S_{\frac{1}{2}}$–$4p^2P_{\frac{3}{2}}$
K I	7699	$4s^2S_{\frac{1}{2}}$–$4p^2P_{\frac{1}{2}}$
Rb I	7800	$5s^2S_{\frac{1}{2}}$–$5p^2P_{\frac{3}{2}}$
Rb I	7948	$5s^2S_{\frac{1}{2}}$–$5p^2P_{\frac{1}{2}}$
Na I	8183	$3p^2P_{\frac{1}{2}}$–$3d^2D_{\frac{3}{2}}$
Na I	8195	$3p^2P_{\frac{3}{2}}$–$3d^2D_{\frac{5}{2}\frac{3}{2}}$
TiO	8432 head, degraded to red	0-0 band of $E^3\Pi$–$X^3\Delta$
Cs I	8521	$6s^2S_{\frac{1}{2}}$–$6p^2P_{\frac{3}{2}}$
CrH	8611 head, degraded to red	0-0 band of $A^6\Sigma^+$–$X^6\Sigma^+$
FeH	8692 head, degraded to red	1-0 band of $A^4\Delta$–$X^4\Delta$
Cs I	8943	$6s^2S_{\frac{1}{2}}$–$6p^2P_{\frac{1}{2}}$
H_2O[a]	~9300	(see text)
VO[a]	~9540–9630	1-0 band of $A^4\Pi$–$X^4\Sigma^-$
FeH	9896 head, degraded to red	0-0 band of $A^4\Delta$–$X^4\Delta$
CrH	9969 head, degraded to red	0-1 band of $A^6\Sigma^+$–$X^6\Sigma^+$

[a]Presence uncertain. See text for details.

REFERENCES

Allard, F. 1998, in Brown Dwarfs and Extrasolar Planets, ed. R. Rebolo, E. L. Martín, & M. R. Zapatero-Osorio (San Francisco: ASP), p. 370

Allard, F., et al. 1998a, in preparation.

Allard, F., Alexander, D.R., Hauschildt, P.H. 1998b, in 10th Cambridge Workshop on Cool Stars, Stellar Systems and the Sun, ed. A. Dupree (San Francisco: ASP), in press

Allard, F., Hauschildt, P.H., Alexander, D.R., & Starrfield, S. 1997, ARA&A, 35, 137

Baraffe, I., Chabrier, G., Allard, F., & Hauschildt, P. H. 1998, A&A, submitted

Basri, G., & Marcy, G. W. 1995, AJ, 109, 762

Bouvier, J., Stauffer, J., Martín, E. L., Barrado y Navascues, D., Wallace, B., & Bejar, V. J. S. 1998, A&A, 336, 490

Becklin, E. E., & Zuckerman, B. 1988, Nature, 336, 656

Bergeron, P., Wesemael, F., Lamontagne, R., Fontaine, G., Saffer, R., & Allard, N. F. 1995, ApJ, 449, 258

Bragaglia, A., Renzini, A., & Bergeron, P. 1995, ApJ, 443, 735

Chabrier, G., & Baraffe, I. 1997, A&A, 327, 1039

Clegg, R. E. S., & Lambert, D. L. 1978, ApJ, 226, 931

Dahn, C. C. 1997, private communication

Delfosse, X., Tinney, C. G., Forveille, T., Epchtein, N., Bertin, E., Borsenberger, J., Copet, E., de Batz, B., Fouqué, P., Kimeswenger, S., Le Bertre, T., Lacombe, F., Rouan, D., & Tiphène, D. 1997, A&A, 327, L25

Engvold, O., Wöhl, H., & Brault, J. W. 1980, A&AS, 42, 209

Henry, T. J., & McCarthy, D. W., Jr. 1993, AJ, 106, 773

Horne, K. 1986, PASP, 98, 609

Iben, I., & Renzini, A. 1983, ARA&A, 21, 271

Iben, I., Tutukov, A. V., & Yungelson, L. R. 1997, ApJ, 475, 291

Jones, H. R. A., Longmore, A. J., Jameson, R. F., & Mountain, C. M. 1994, MNRAS, 267, 413

Jones, H. R. A., & Tsuji, T. 1997, ApJ, 480, L39

Jørgensen, U. G., Jensen, P., & Sørensen, G. O. 1994, in Molecular Opacities in the Stellar Environment, ed. P. Thejll & U. Jørgensen (Copenhagen: Nordita), 51

Keenan, P. C. 1957, PASP, 69, 5

Keenan, P. C., & Schroeder, L. W., 1952, ApJ, 115, 82

Kirkpatrick, J. D., Henry, T. J., & Irwin, M. J. 1997, AJ, 113, 1421

Kirkpatrick, J. D., Henry, T. J., & Liebert, J. 1993a, ApJ, 406, 701

Kirkpatrick, J. D., Kelly, D. M., Rieke, G. H., Liebert, J., Allard, F., & Wehrse, R. 1993b, ApJ, 402, 643

Kroupa, P. 1998, in Brown Dwarfs and Extrasolar Planets, ed. R. Rebolo, E. L. Martín, & M. R. Zapatero-Osorio (San Francisco: ASP), p. 483

Lindgren, B., & Olofsson, G. 1980, A&A, 84, 300

Martín, E. L., Basri, G., Delfosse, X., & Forveille, T. 1997, A&A, 327, L29

Oke, J. B. 1974, ApJS, 27, 21

Oke, J. B. 1990, AJ, 99, 1621

Oke, J. B., Cohen, J. G., Carr, M., Cromer, J., Dingizian, A., Harris, F. H., Labrecque, S., Lucinio, R., Schaal, W., Epps, H., & Miller, J. 1995, PASP, 107, 375

Oppenheimer, B. R., Kulkarni, S., Matthews, K., & van Kerkwijk, M. H. 1998, ApJ, submitted

Partridge, H. & Schwenke, D. W. 1997, J. Chem. Phy., 106, 4618

Pearse, R. W. B., & Gaydon, A. G. 1963, The Identification of Molecular Spectra, 3rd ed. (New York: John Wiley & Sons), p. 148

Phillips, J. G., Davis, S. P., Lindgren, B., & Balfour, W. J. 1987, ApJS, 65, 721

Reid, I. N. 1996, AJ, 111, 2000

Ruiz, M. T., Leggett, S. K., & Allard, F. 1997, ApJ, 491, L107

Saffer, R. A., Livio, M., & Yungelson, L. R. 1998, ApJ, in press

Sauval, A. J. 1978, A&A, 62, 295

Segretain, L., Chabrier, G., Hernanz, M., Garcia-Berro, E., Isern, J., & Mochkovitch, R. 1994, ApJ, 434, 641

Scalo, J. M. 1986, Fund. of Cosmic Phy., 11, 1

Schiavon, R. P., Barbuy, B., & Singh, P. D. 1997, ApJ, 484, 499

Schultz, A. B., et al. 1998, ApJL, 492, L181

Schwenke, D. W. 1998, private communication

Sharp, C. M., & Huebner, W. F. 1990, ApJS, 72, 417

Spinrad, H., & Wing, R. F. 1969, ARA&A, 7, 249

Stockton, A. 1996, private communication

Thackrah, A., Jones, H., & Hawkins, M. 1997, MNRAS, 284, 507

Tinney, C. G. 1998a, in Brown Dwarfs and Extrasolar Planets, ed. R. Rebolo, E. Martín, M. R. Zapatero Osorio (San Francisco: ASP), p. 75

Tinney, C. G. 1998b, MNRAS, submitted

Tinney, C. G., Delfosse, X., & Forveille, T. 1998b, ApJ, 490, L95

Tinney, C. G., Mould, J. R., & Reid, I. N. 1993, AJ, 105, 1045

Tsuji, T., Ohnaka, K., & Aoki, W. 1996, A&A, 305, L1

Weidemann, V. 1987, A&A, 188, 74

Wing, R. F., Cohen, J., & Brault, J. W. 1977, ApJ, 216, 659

Zuckerman, B., & Becklin, E. E. 1992, ApJ, 386, 260

This 2-column preprint was prepared with the AAS LaTeX macros v4.0.

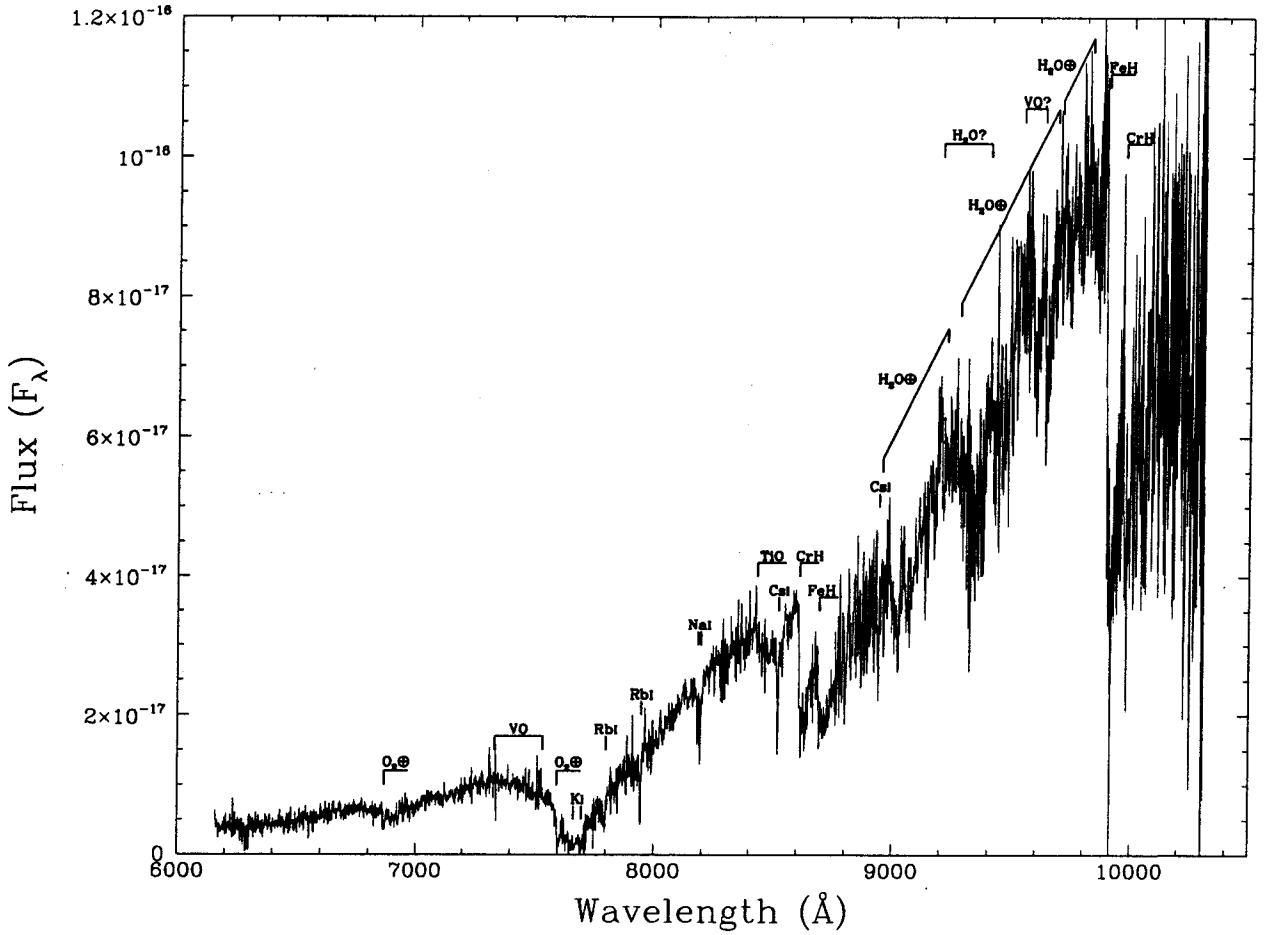

Fig. 1.— The optical spectrum of GD 165B. The units of F_λ are erg/cm^2·s·Å. The spectrum has not been corrected for the effects of telluric absorption, so the A- and B-bands of O_2 are still present as are terrestrial H_2O bands longward of 9000 Å.

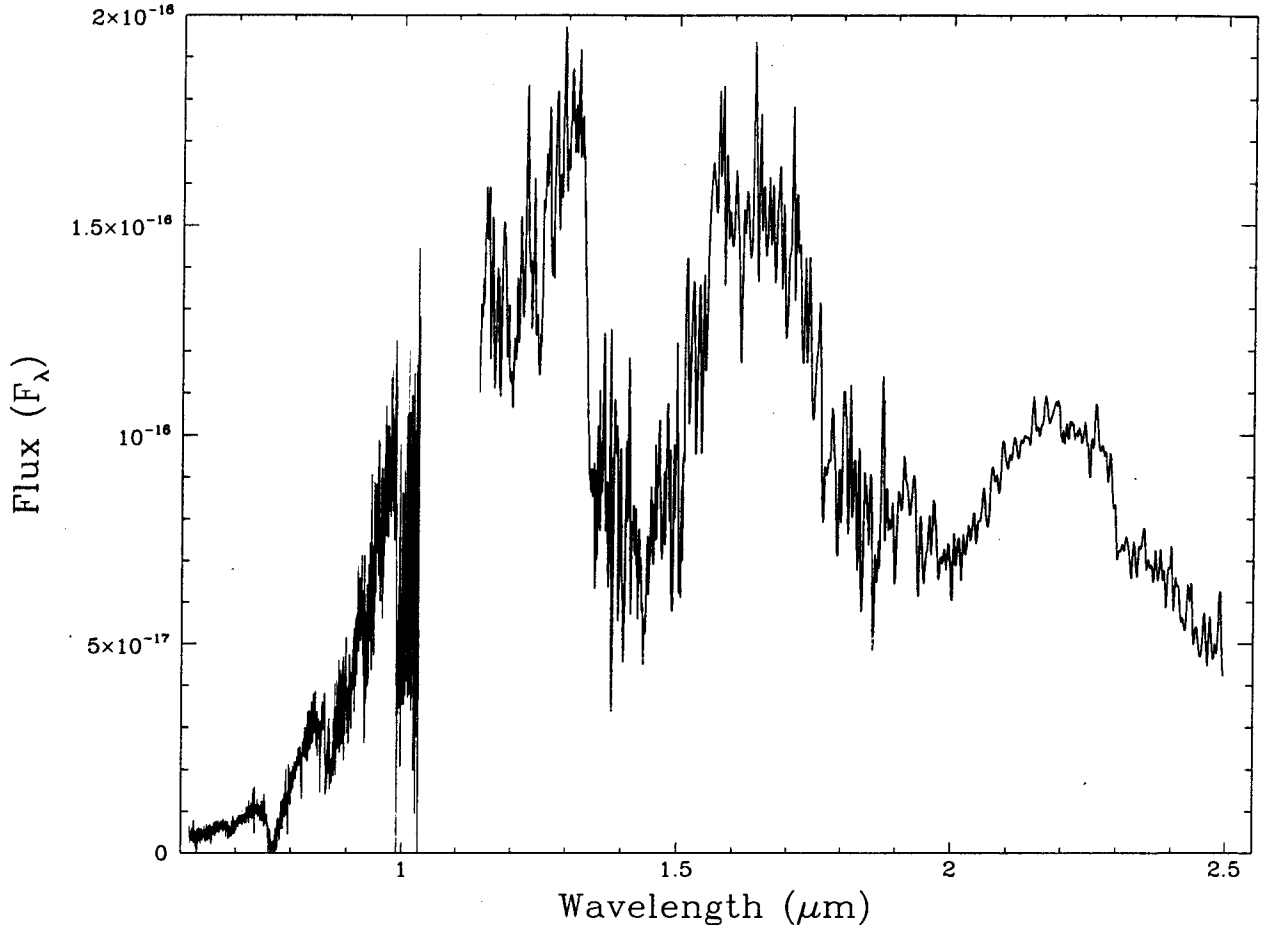

Fig. 2.— The spectrum of GD 165B from the optical through the near-infrared. The units of F_λ are erg/cm^2·s·Å. The optical portion is the same as that shown in Figure 1 and the near-infrared portion is from Jones et al. 1994. Unlike the optical spectrum, the near-infrared portion has been corrected for telluric absorption. The relative normalizations between the two pieces has been adjusted to agree with published IJHK photometry.

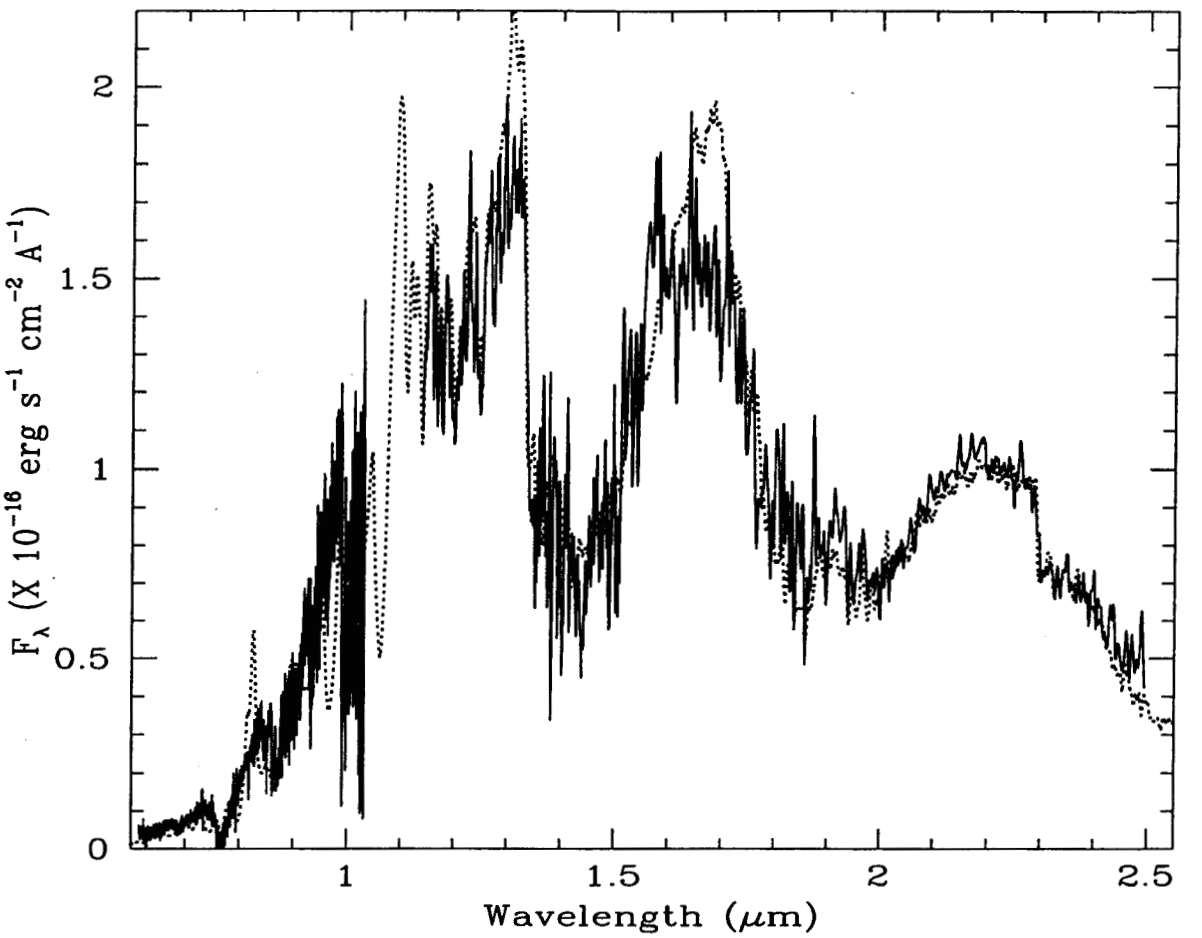

Fig. 3.— Best fit of the NextGen-dusty models (Allard et al. 1998a, 1998b) to the observed spectrum of GD 165B. The model (T_{eff}=1900K, log(g)=5.0 — dotted line) has been convolved with a Gaussian instrumental response of 30 Å FWHM, and is normalized to the observed spectrum (full line) at 1.2 μm. The quality of this fit is unprecedented. Models without dust grains (especially iron, forsterite and $Ca_2Al_2SiO_7$) underpredict the emergent J-to-K band flux by as much as 2 magnitudes.

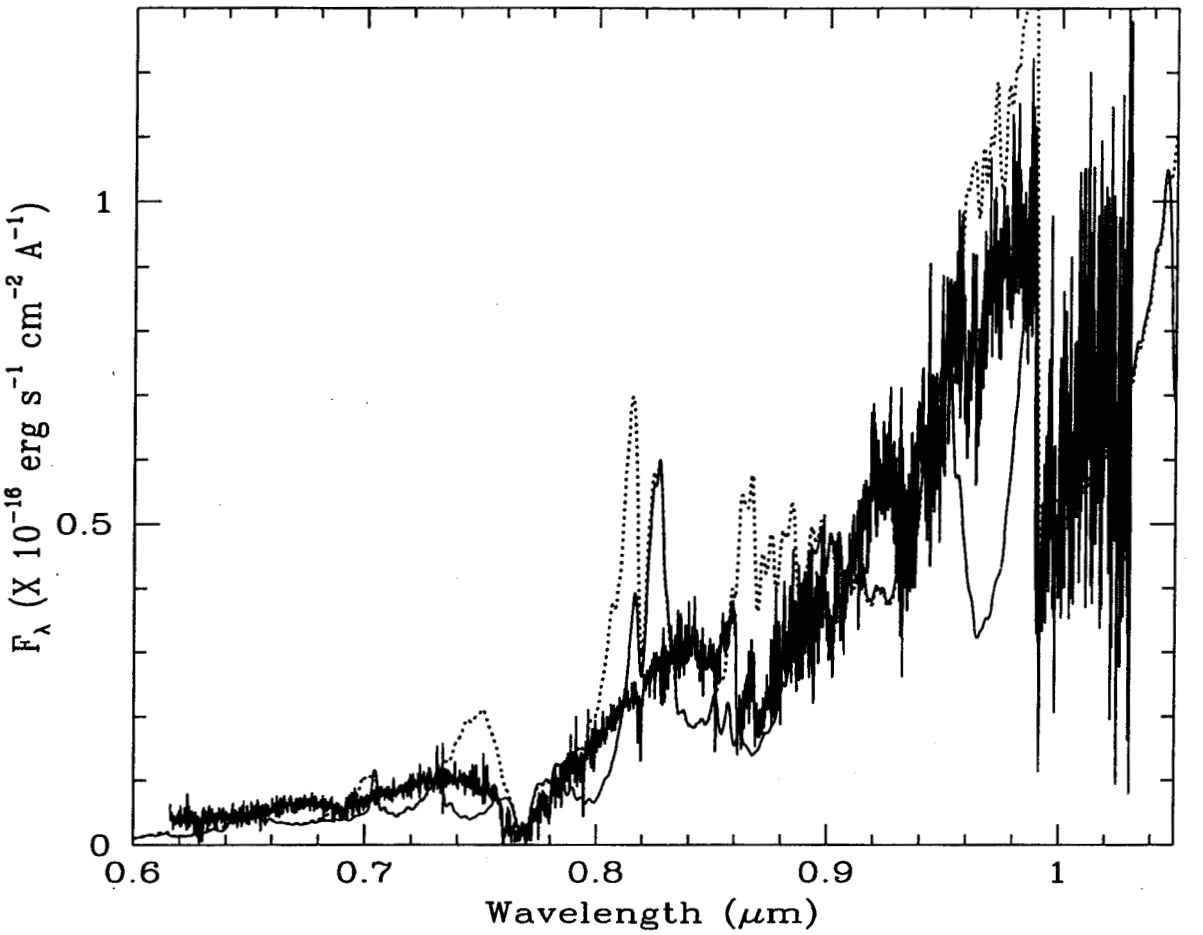

Fig. 4.— Same fit as in Figure 3, but showing the optical spectral region in more detail. The adopted T_{eff}=1900K, log(g)=5.0 model (lighter solid line) is also compared with a synthetic spectrum where VO band opacities are arbitrarily neglected (dotted line). The models are shown with a resolution of 12 Å. While the adopted model obviously underpredicts the depletion of TiO and VO in the atmosphere of GD 165B, the comparison shows that those bands have still not fully disappeared.

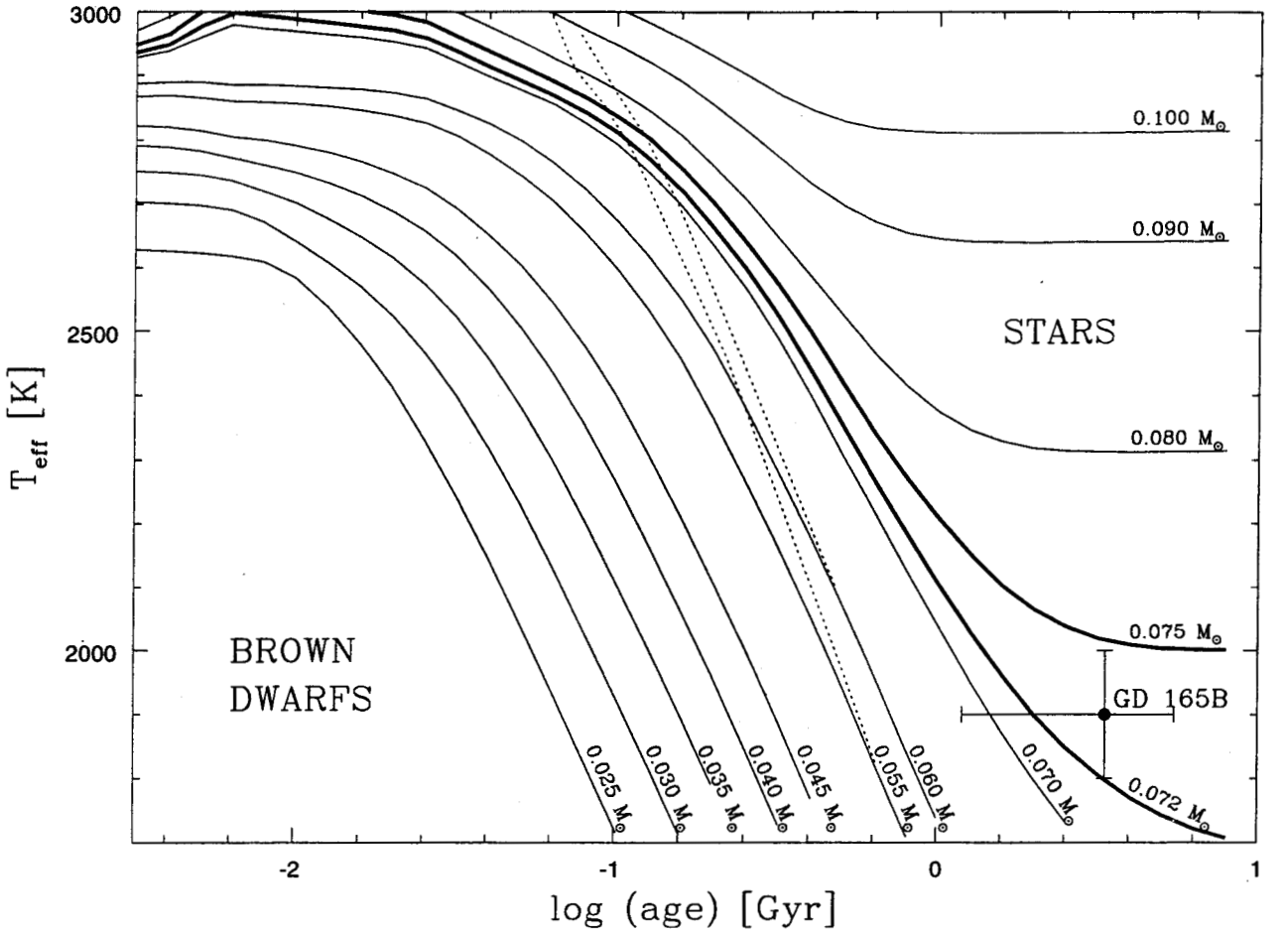

Fig. 5.— The position of GD 165B on the T_{eff} vs. age plane along with the most recent theoretical models of Chabrier & Baraffe (1997) and Baraffe et al. (1998) for solar metallicity ([M/H] = 0). The transition region between stars and brown dwarfs falls between the two heavy lines. The dashed lines mark the locus of lithium depletions of $Li/Li_o = 0.5$ (to the left) and 0.01 (to the right). Based on its position in this diagram, GD 165B is either a transition object or a brown dwarf.

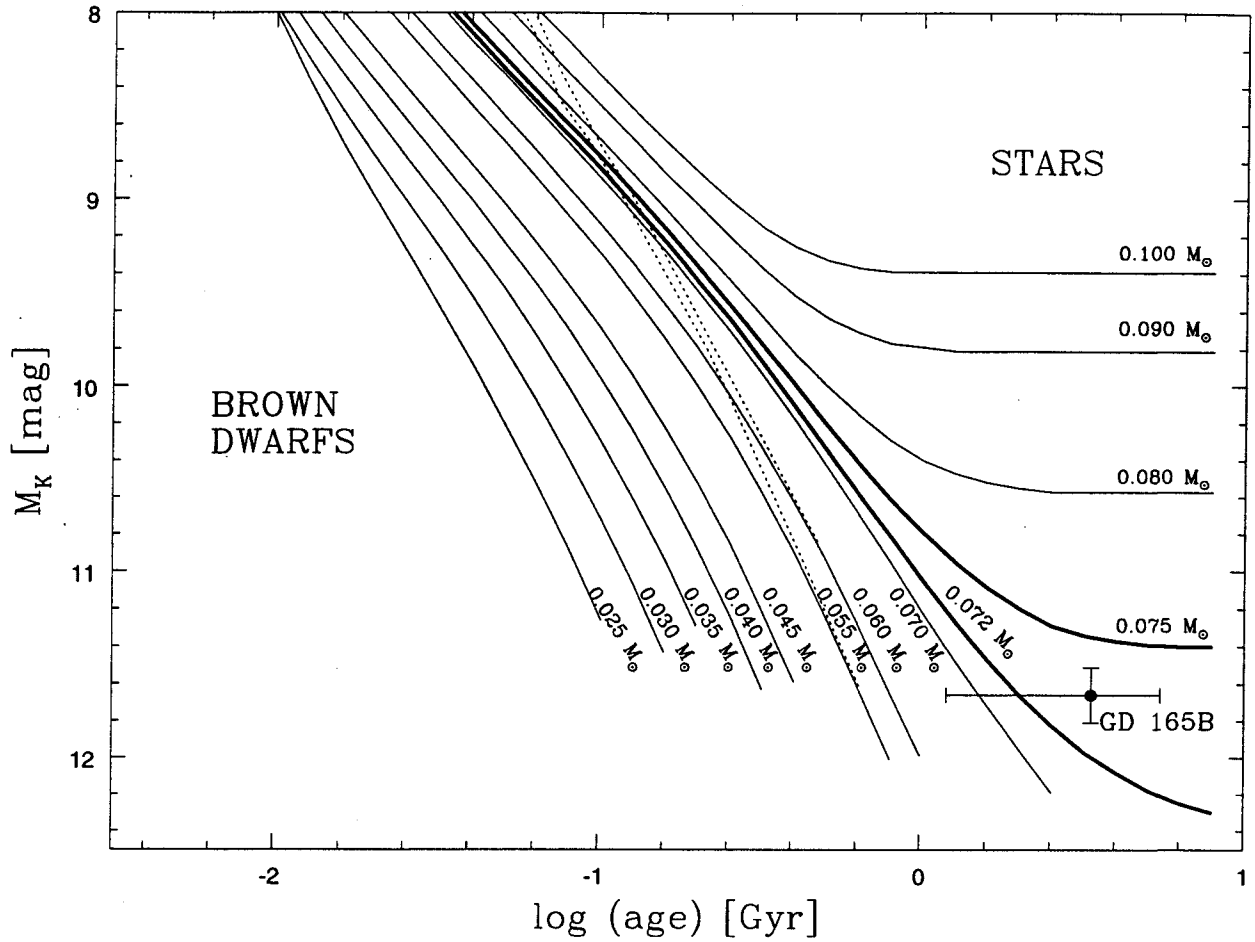

Fig. 6.— The position of GD 165B on the M_K vs. age plane. See the caption to Fig. 5 for details.